Available online at www.sciencedirect.com
SCIENCE DIRECT®
Pergamon
Cement and Concrete Research 33 (2003) 1417–1422
CEMENT AND CONCRETE RESEARCH

Alkali-activated cement based on natural SiO_2-containing material Part I. Strength, hydration, microstructure and durability

C. Freidin*

Unit of Desert Architecture and Urban Planning, Department of Man in the Desert, The Jacob Blaustein Institute for Desert Research, Ben-Gurion University of the Negev, Sede-Boqer Campus, Negev 84990, Beer-Sheva, Israel

Received 17 July 2002; accepted 25 February 2003

Abstract

An alkali-activated cement (AAC) based on natural SiO_2-containing materials—grounded porcellanite (Pr) and highly dispersed pure quartz sand—was examined. Sodium hydroxide was used as an alkali activator. The pressed specimens were prepared and were cured in an autoclave at a pressure of 1.6 MPa and a temperature of 205 °C. It was shown that the strength of cement as well as compound and the microstructure of its hydration products depend on the cement composition. It was distinguished that autoclave-cured cementing matter comprises secondary quartz and the mass of sodium hydrated silicates along with the initial Pr crystal phases. After a 2-year storage under water, 15% Na_2SO_4, and Dead Sea water, the strength of specimens decreased by 17.5–20%. Control specimens, prepared with Portland cement and immersed in a 15% Na_2SO_4 solution for 2 weeks, were broken up completely. Positive results of long-term durable tests suggest that an AAC based on natural raw material would be stable in other salt solutions.

Keywords: Alkali-activated cement; Mechanical properties; Hydration product; Durability

1. Introduction

Alkali-activated cement (AAC) utilizes industrial by-products such as slag, fly ash, and others [1–7]. It was also reported to have superior durability in aggressive conditions as compared to Portland cement [8–10]. A promising, chemically resistant cement is quartz bond, which is generated in a raw material system including high-silica alkaline glass, highly dispersed pure quartz sand, and water [10]. Freidin [11] and Freidin and Sedykh [12] developed many technological aspects and peculiarities of manufacturing chemical-resistant silica concrete (SC) using this type of cement. Further investigations suggested the possibility of substituting very expensive high-silica alkaline glass with the product of baking the mixture of quartz sand and 0.7 wt.% alkali metal hydroxide or carbonate at 1000–1550 °C [13]. As a result, the quartz is entirely converted into X-ray amorphous, intermediate phase and into a metastable cristabalite having a tridimite impurity.

The analysis of the recent geochemical and mineralogical data showed that there is a natural SiO_2-containing material, porcellanite (Pr), containing cristabalite and tridimite in opal CT [14,15]. Pr is a diagenetic rock. It occurs in both lithified and unconsolidated sediments. Pr concretions and deposits are apparent in various oceans and on land in USA, Ireland, Israel, Australia and other countries. It was found that Pr is dissolved in alkali solutions (sodium hydroxide or sodium carbonate), obtaining a solution of sodium silicate–water glass [16].

In our opinion, secondary quartz can settle at certain temperature and pressure conditions from the sodium silicate solution with particles of crystal silica seed (CSS)—fine crystal quartz—especially added to Pr. In this way, an AAC could be obtained from Pr.

The effect of the alkali activator, the ratio of Pr to CSS quantity (Pr/CSS) and the particle sizes of grounded Pr on strength as well as on the composition and microstructure of new formations of AAC are discussed. Moreover, certain aspects of durability of AAC under long-term exposure to water, sodium sulphate solution, or Dead Sea water (DSW) are considered.

* Tel.: +972-8-659-6876; fax: +972-8-659-6881.
E-mail address: freidin@bgumail.bgu.ac.il (C. Freidin).

0008-8846/03/$ – see front matter © 2003 Elsevier Ltd. All rights reserved.
doi:10.1016/S0008-8846(03)00088-7

2. Materials

2.1. Pr

Samples of Pr were obtained from Mishash Formation (Negev, Israel). The chemical composition of Pr is (%) as follows: SiO_2-65.2; Al_2O_3-1.3; Fe_2O_3-0.6; CaO-11.3; MgO-0.8; TiO_2-0.1; SO_3-2.7; P_2O_5-3.9; Na_2O-1.3; K_2O-0.2; F-0.35; Cl-3.2; $LOI_{950\ ^\circ C}$-11.2. The specific gravity of Pr is 2200 kg m^{-3}. Visual observations, optical microscopy, X-ray diffraction (XRD) and scanning electronic microscopy (SEM) investigations showed that opal CT containing cristabalite and tridimite is the main constituent of Pr (see Fig. 1). Other minerals are microquartz, calcite, dolomite, and minor fluorapatite. Clays, humic acid and fulvic acid are presented in minor quantities.

Pr was prebroken in a jaw crusher, screened, milled, and used as a fraction <0.63 and 0.63–1.18 mm.

CSS was prepared by milling natural high quartz sand (S). The fineness of grinding was 320–330 m^2 kg^{-1} (after Blaine), as defined in ASTM 204.

2.2. Alkali activator

Chemical purity grade sodium hydroxide was used as an AAC. AAC was dissolved in water and added in AAC, together with mixing water.

2.3. Water

Common tap water was used for mixing water and for long-term water exposure tests.

3. Methods

AAC was prepared by premixing ground Pr and dispersed CSS. AAC was dissolved in water and added to AAC, together with mixing water. The mixtures were blended by hand for 3–5 min to obtain a homogeneous mass. The data concerning the mixture compositions of test specimens and curing conditions are shown in Table 1.

Cylinders of 3.0 cm in height and 5.7 cm in diameter served as test AAC specimens. The specimens were molded

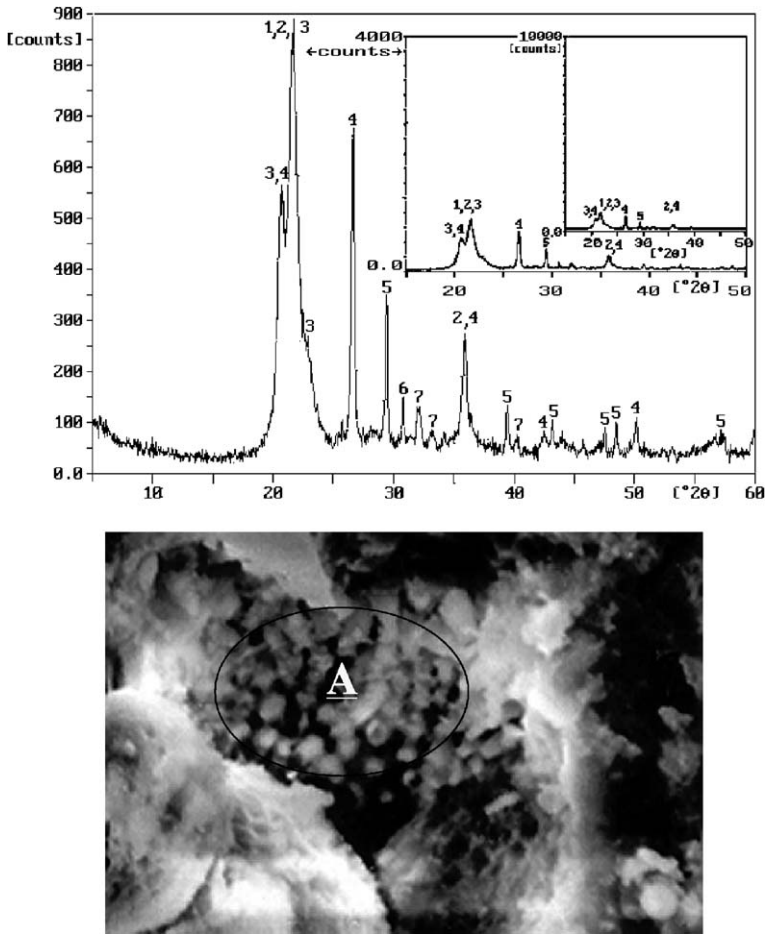

Fig. 1. Results of XRD and SEM analyses of Pr. Upper: XRD patterns in different scales: (1) opal; (2) cristabalite; (3) tridimite; (4) quartz; (5) calcite; (6) dolomite; and (7) fluorapatite. Down: SEM micrograph (magnification $\times 3600$); A—spherolites of cristabalite.

Table 1
Compositions of specimens and curing conditions

	Unit	Batch number			
		1	2	3	4
Mixture composition					
Pr	Weight part	0.6–2.0	0.2–2.0	1	1
CSS–S	Weight part	1	1	1	1
Alkali activator (AAC)	% by weight (from mass of Pr+CSS)	2–12	8	8	8
Moisture	% by weight (from mass of Pr+CSS+AAC)	15	15	15–11	12
Curing conditions (autoclave, P= 1.6 MPa, T= 205 °C)					
t=5 h		+	+	+	–
t=21 h		–	–	+	+

Compositions of specimens of Batches 1–3 contained milled Pr as a fraction <0.63 mm; a portion of specimens of Batch 3 was prepared from mixtures in which Pr grains with sizes <0.63 mm were substituted by particles with sizes of 0.63–1.18 mm.
Specimens of Batch 4 were prepared using PrB including 60% Pr (by weight) with grain sizes <0.63 mm and with a 40% Pr of fraction of 0.63–1.18 mm.

on a Carver laboratory hand press at a compaction pressure of 20 MPa and cured in the laboratory autoclave at a steam pressure of 1.6 MPa and a temperature of 205 °C. The specimens were crush-tested to determine the initial compressive strength and compressive strength throughout a certain period. The small pieces of tested specimens were examined by XRD analysis and SEM to find the composition and structure for new formations of the cementing matter of AAC.

After curing, the specimens of Batch 4 were kept in various media (water, 15% sodium sulphate solution, or DSW, containing 15% KCl+40% $MgCl_2$+8% NaCl) at room temperature for 2 years. The choice of these durability test conditions was determined by the necessity to defend the potential of AAC as a binder under the long-term action of neutral and salt liquid. Every 3–6 months, the specimens were removed from the test solution, inspected visually, and crushed to check the changes in the form and strength of AAC.

4. Results and discussion

4.1. Influence of alkali activator amount on strength of AAC

It can be seen from Fig. 2 that an increase of AAC amount raised the compressive strength independently of Pr/CSS in AAC. In the interval of 2–6% AAC content, a quick rise in strength was observed. When AAC amount was greater than 6%, the specimens' strength was increased gradually and the strength–development curves could be described as exponential.

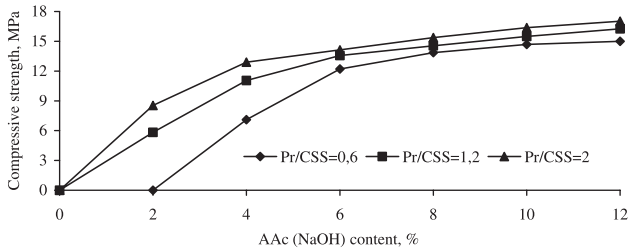

Fig. 2. Compressive strength of AAC vs. alkali activator content.

In Fig. 3, XRD patterns for AAC with Pr/CSS=0.6 and AAC=4–12% are presented. These patterns are similar to the ones that were obtained in experiments with other Pr/CSS ratios. They give a possibility to retrace the changes in curing products that were due to varying quantities of AAC. When AAC amount was 4%, the crystal phase of new formations consisted of calcite (5), quartz (4), opal (1), cristabalite (2) and tridimite (3). The high intensity of calcite peak (5) can be attributed to a redistribution of the relative content of crystal phases in favor of calcite, which is a result of partially dissolving opal, cristabalite, as well as tridimite. The intensity of XRD peaks (1)–(3) is less than for the initial Pr, which could be explained by the changes in their liquid phase of curing system and the formation of sodium-hydrated silicates. However, the presence of sodium-hydrated silicates as an independent crystal phase in cured AAC was not detected on the XRD pattern through their X-ray amorphousness.

The evidences for the presence of sodium-hydrated silicates as well as the secondary quartz were obtained by SEM. These products can be seen in Fig. 4.

The increase of AAC amount to 8–12% lowered the content of opal (1), cristabalite (2), tridimite (3), and calcite

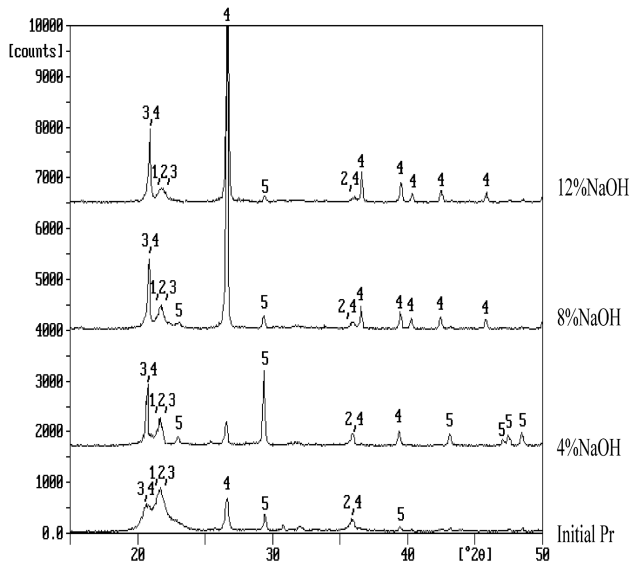

Fig. 3. XRD patterns of autoclave-cured ACC and initial Pr: (1) opal; (2) cristobalite; (3) tridimite; (4) quartz; and (5) calcite.

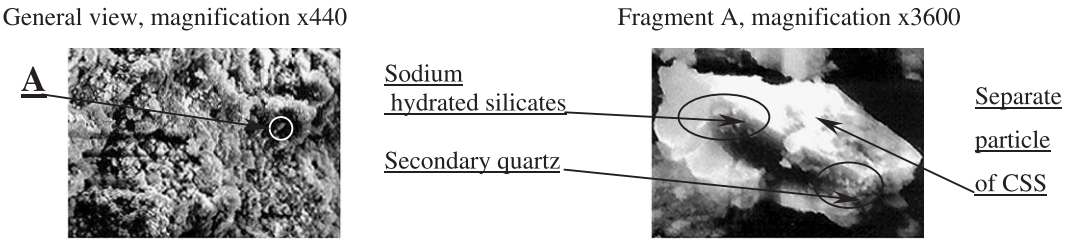

Fig. 4. SEM micrograph of autoclave-cured ACC.

(5), and improved the crystallization of quartz, which was reflected on XRD patterns as peaks (4) with high intensity.

4.2. Effect of Pr/CSS ratio on the strength and coefficient of softening of AAC

From Fig. 5, it follows that the compressive strength of specimens was increased at all times when the Pr/CSS ratio in AAC was brought to 2.0. The strength–development curves have two parts. Corresponding to the first part, AAC strength increased rapidly as the Pr/CSS ratio reached 0.6–0.9. The second part had an almost straight line appearance for specimens with Pr/CSS ratios from 0.6 to 0.9–2.0. In this case, strength was increased slightly.

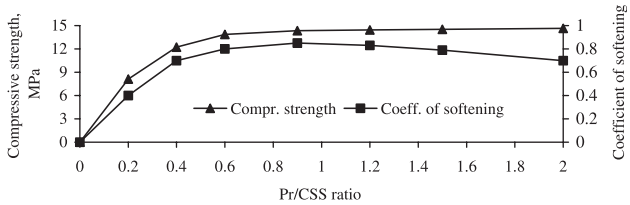

Fig. 5. Effect of Pr/CSS ratio on mechanical properties of AAC.

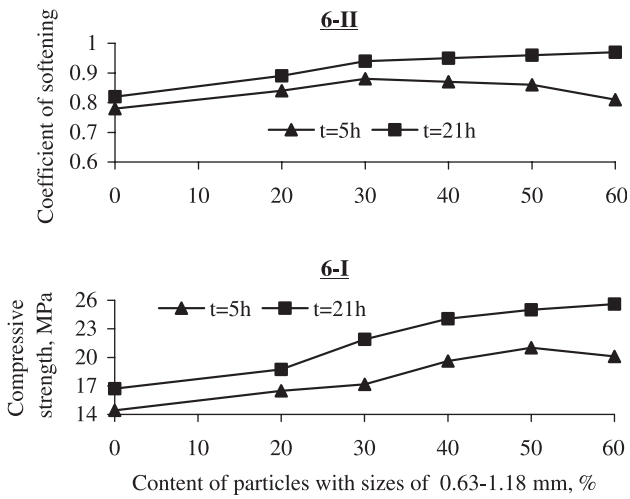

Fig. 6. Compressive strength and coefficient of softening of AAC vs. content of particles of 0.63–1.18 mm in Pr. 6-I: Compressive strength; 6-II: Coefficient of softening.

The CS curve had the inflection point at a Pr/CSS ratio of 0.9. The magnitude of CS at this point was 0.85, which is a very remarkable index for binders. The next reduction of CS is probably connected with a partial dissolution of sodium hydrate silicates (one of the least tolerant of curing products of AAC to water), the quantities of which were increased as Pr/CSS ratio was increased.

Any changes or additional peaks for the new curing product, which should have appeared at increased Pr/CSS ratios from 0.2 to 2.0, were not displayed in XRD patterns. XRD patterns were similar to the XRD pattern for AAC with 8% NaOH (see Fig. 3).

4.3. Effect of fraction composition of Pr on the strength and coefficient of softening of ACC

Curves showing the change of compressive strength and CS of autoclave-cured AAC at the partial substitution of Pr constituent part with dimension <0.63 mm by particles with sizes of 0.63–1.18 mm are presented in Fig. 6. The curve of compressive strength of AAC cured in autoclave for 5 h vs.

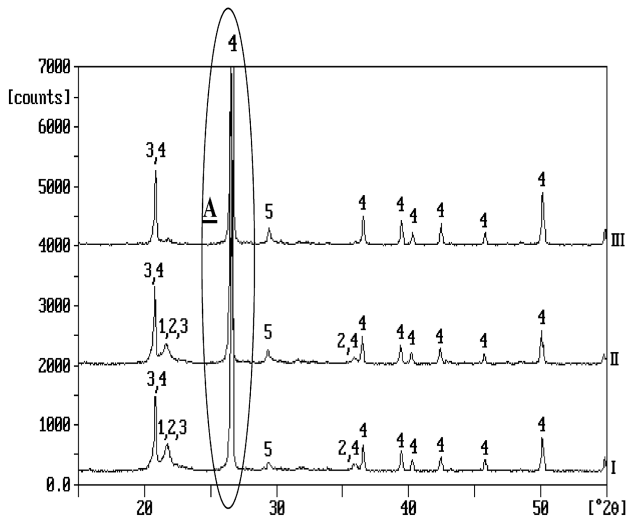

Fig. 7. XRD patterns of autoclave-cured ACC (for explanation, see Fig. 3). (I) ACC:Pr component—fraction <0.63 mm; curing time $t=5$ h. (II)ACC:Pr component—50% fraction <0.63 mm + 50% fraction of 0.63–1.18 mm; curing time $t=5$ h. (III) ACC:Pr component—fraction <0.63 mm + 50% fraction of 0.63–1.18 mm; curing time $t=21$ h.

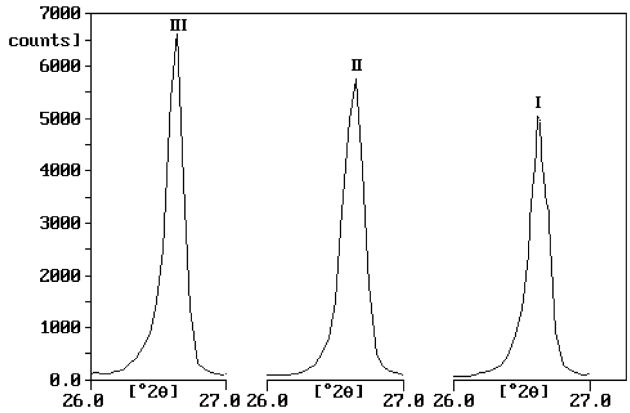

Fig. 8. Intensity of quartz peaks 4 at an angle of 2θ = 26.65° on XRD patterns (Fragment A). I-ACC: Pr component-fraction less than 0.63 mm, curing time t=5h; II-ACC: Pr component-fraction less than 0.63 mm−50% + Pr component-fraction less than 0.63 mm, curing time t=5h; III-ACC: Pr component-fraction less than 0.63 mm−50% + Pr component-fraction less than 0.63 mm, curing time t=21h.

the content of fraction of 0.63–1.18 mm had the point of inflection at 50% content, after which strength decreased (Fig. 6I). Something similar was detected for the curve of CS = *f* (fraction of 0.63–1.18 mm content), but the inflection point was obtained at 30% content of fraction of 0.63–1.18 mm (Fig. 6II). An increase of autoclave curing up to 21 h changed this regularity. A continuous increase of compressive strength as well as CS was observed when the content of fraction of 0.63–1.18 mm in Pr increased up to 60%.

The changes, which took place in the composition and structure of AAC curing products at the replacement of Pr component with sizes less than 0.63 mm by 50% 0.63- to 1.18-mm fractions, can be followed in Figs. 7–9. As can be concluded from Fig. 7, the XRD pattern of AAC, based on the Pr component containing 50% (by weight) fraction of those < 0.63 mm and 50% fraction of those 0.63–1.18 mm (Curve 2), is very close to the one of AAC prepared only from Pr with particles sizes < 0.63 mm (Curve 1) at a curing time of 5 h. In both cases, the composition of the crystal phase of new formations is identical to that given in Section 4.1 and Fig. 3. But the intensity of the quartz peak at an angle of 2θ = 26.65° in the XRD pattern of AAC-containing particles with sizes of 0.63–1.18 mm (Fig. 8, Curve 2) is higher than that of AAC without this fraction (Fig. 8, Curve 1). This indicates a better crystallization of the secondary quartz, which is a result of an involvement of coarse 0.63- to 1.18-mm particles in AAC curing processes (compare micrographs 1 and 2; Fig. 9). The crystallization of the secondary quartz was improved when the period of autoclave curing of AAC containing 0.63- to 1.18-mm particles was increased up to 21 h. Fig. 8 (Curve 3) and Fig. 9 (micrograph 3) illustrate this effect.

4.4. Durability of AAC

The development of the compressive strength of AAC specimens placed in water, sodium sulfate solution and DSW is shown in Fig. 10. For up to 3 months, strength reduction did not exceed 11.7–15%. After that—up to 12 months—strength reduction decreased to 3.3–4.5%. When the exposure period of specimens increased from 12 to 24 months, the strength remained practically unchanged and at the 24th month, it was 80.0–82.5% from the starting value (i.e., strength reduction was 17.5–20.0%). Lesser strength value was related to specimens of water exposure and the greatest strength was related to specimens immersed in the Na_2SO_4 solution. The DSW storage specimens were intermediate in strength between water and sodium sulphate solution specimens.

Visual inspections showed that at the end of the durable tests, the specimens had no visible deterioration and traces of corrosion (cracks, corner chipping, etc.) compared to their initial states.

Considering the mechanism of long-term action of test media under immersed conditions, it should be emphasized that no chemical interaction between these liquids and the components of cured AAC, including the cementitious bond, was detected. At long-term immersion, mainly two physical processes seemed to effect the AAC: permeation of cured products by the liquid medium and their "softening"

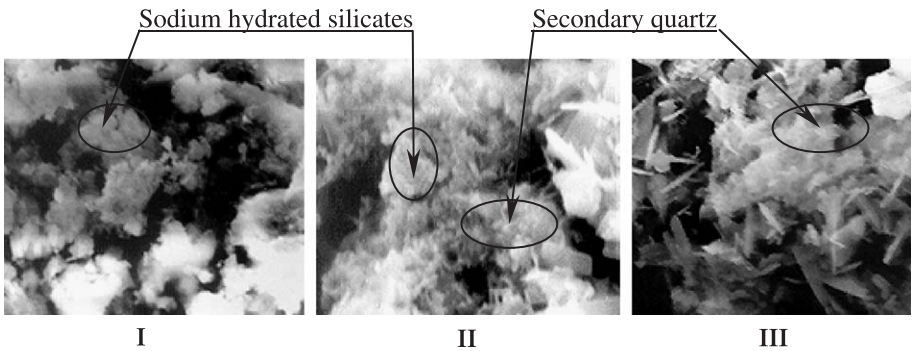

Fig. 9. SEM micrograph of cured AAC. For explanations, I-ACC: Pr component-fraction less than 0.63 mm, curing time t=5h; II-ACC: Pr component-fraction less than 0.63 mm−50% + Pr component-fraction less than 0.63 mm, curing time t=5h; III-ACC: Pr component-fraction less than 0.63 mm−50% + Pr component-fraction less than 0.63 mm, curing time t=21h.

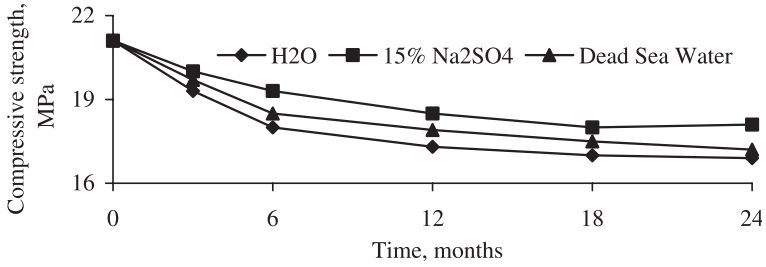

Fig. 10. Compressive strength of AAC on long standing in various liquid media.

that resulted in strength reduction. The dynamics and value of strength reduction depend on the speed and depth of permeation, which were in turn a function of the density and viscosity of the permeating fluid. The fluids used in experiments fall into a specific order according to these indexes. Water had the least density and viscosity, whereas the sodium sulphate solution is characterized by the highest density and viscosity. Respectively, water permeated in AAC specimens faster and deeper than sulphate solution and DSW, which are more viscous. Correspondingly, the compressive strength of specimens emerging in water decreased faster and to a greater degree than those kept in sodium sulphate solution and DSW.

It should be noted that the reference specimens of mortar with a Portland cement/sand ratio of 1:2.5 and a w/c ratio of 0.35, stored in 15% Na_2SO_4, were broken up completely during 2 weeks.

5. Conclusions

The main conclusions extracted from this work are:

1. Long-lived AACs of autoclave curing can be prepared on the basis of the natural raw material Pr (containing active SiO_2 in the form of opal, cristabalite and tridimite) and CSS (highly dispersed pure quartz sand). Hydroxide sodium is an AAC of a binder.
2. The strength and CS of AAC depend on composition binder and content of Pr coarse particles with sizes of 0.63–1.18 mm, as well as on the duration of autoclave curing.
3. The cementing matter of autoclave curing AAC can contain new formations in the form of secondary quartz, and the mass of sodium-hydrated silicates along with the initial crystal phases (calcite, quartz, opal, cristabalite and tridimite) of Pr can be determined.
4. Long-term storage of specimens under water, 15% sodium sulfate solution, or DSW (15% KCl + 40% $MgCl_2$ + 8% NaCl) showed 17.5–20% decreases in the strength of AAC after 2 years of tests. Control specimens, prepared with Portland cement and immersed into a 15% Na_2SO_4 solution for 2 weeks, were broken up completely.
5. Positive results of long-term durable tests suggest that AAC made from Pr would be stable in other salt solutions.

References

[1] F. Puertas, S. Martinez-Ramirez, S. Alonso, T. Vazquez, Alkali-activated fly ash/slag cements: strength behavior and hydration products, Cem. Concr. Res. 30 (2000) 1625–1632.
[2] Z. Xie, Y. Yuping, Hardening mechanisms of an alkaline-activated class F fly ash, Cem. Concr. Res. 31 (2001) 1245–1249.
[3] A. Palomo, M.W. Grutzeck, M.T. Blanco, Alkali-activated fly ashes. A cement for the future, Cem. Concr. Res. 29 (1999) 1323–1329.
[4] D.M. Roy, Alkali-activated cements. Opportunities and challenges, Cem. Concr. Res. 29 (1999) 249–254.
[5] S.D. Wang, X.C. Pu, K.L. Scrivener, P.L. Pratt, Alkali-activated cement and concrete. A review of properties and problems, Adv. Cem. Res. 7 (1995) 93–102, 527.
[6] P.V. Krivenko, Alkaline cements, Proceedings of 9th International Congress on the Chemistry of Cement, New Delhi, 1992, pp. 482-488.
[7] V.D. Glukhovskij, Y. Zaitsev, V. Pakhomow, Slag–alkaline cements and concretes structures, properties, technological and economical aspects of the use, Silic. Ind. 10 (1983) 197–200.
[8] T. Bakharev, J.G. Sanjayan, Y.B. Cheng, Sulfate attack on alkali-activated slag concrete, Cem. Concr. Res. 32 (2002) 211–216.
[9] W. Jiang, M.R. Silsbee, E. Breval, D.M. Roy, Alkali-activated cementitious materials in chemically aggressive environments, Proceedings of the Materials Research Society Symposium on "Mechanical and Chemical Degradation Cement-Based Systems", E&FN Spon, Materials Research Publisher, London, UK, 1997, pp. 289–296.
[10] V.P. Kirilishin, Silica Concrete, Budivelnik, Kiev, 1975, in Russian.
[11] C. Freidin, Stability of silica–concrete based on quartz bond in water, sodium sulfate and sulphuric acid solutions, Br. Ceram. Trans. 100 (2001) 129–133.
[12] C. Freidin, U. Sedykh, Application of Silica Concrete in Power Plant Construction, Informenergo, Moscow, 1982, in Russian.
[13] V.P. Kirilishin, Binder for chemically resistant concrete, USSR Patent, 1980 (in English), CODEN: USXXAM US 4234347 19801118, Application: US 79-71056 19790830, CAN 94:89176, AN 1981:89176, CAPLUS.
[14] Y. Kolodny, Y. Nathan, E. Sass, Porcellanite in the Mishash Formation, Negev, Southern Israel, J. Sediment. Petrol. 35 (1965) 454–463.
[15] Y. Kolodny, Lithostratigraphy of the Mishash Formation, Northern Negev, Israel J. Earth Sci. 16 (1967) 57–73.
[16] I. Alexander, Manufacture of pure silica from rock containing it, Israel Patent 104,584, 1998.